

Highlights

Reducing RES Droughts through the integration of wind and solar PV

Boris Morin, Aina Maimó Far, Damian Flynn, Conor Sweeney

- RES droughts are analysed using 45 years of hourly wind and solar PV generation data
- RES droughts from C3S-Energy and ERA5-Atlite datasets are compared
- Adding solar PV to a wind-dominated system reduces RES drought frequency and duration
- Validated RES datasets are crucial to accurately identify RES drought extremes

Reducing RES Droughts through the integration of wind and solar PV

Boris Morin^{a,*}, Aina Maimó Far^a, Damian Flynn^b, Conor Sweeney^a

*^aSchool of Mathematics and Statistics, University College Dublin, Belfield, Dublin
4, Dublin, D04 V1W8, Ireland*

*^bSchool of Electrical and Electronic Engineering, University College Dublin, Belfield,
Dublin 4, Dublin, D04 V1W8, Ireland*

*Corresponding author

Email addresses: `boris.morin@ucdconnect.ie` (Boris Morin),
`aina.maimofar@ucd.ie` (Aina Maimó Far), `damian.flynn@ucd.ie` (Damian Flynn),
`conor.sweeney@ucd.ie` (Conor Sweeney)

Abstract

Increasing the share of electricity produced from renewable energy sources (RES), combined with RES dependence on weather, poses a critical challenge for energy systems. This study investigates the importance of the balance between wind and solar photovoltaic (PV) capacity on periods of low renewable generation, known as RES droughts. Three different RES datasets are used to estimate the capacity factors for different scenarios of installed capacities for wind and solar PV power. The skill of the RES datasets is quantified by comparing capacity factor time series to observed hourly data and by assessing their representation of observed RES droughts. The RES datasets are used to generate a 45-year hourly time series of RES capacity factor, enabling analysis of the frequency, duration and return periods of RES droughts at a climatological scale. Results show the importance of using an accurate, validated RES dataset for RES drought risk assessment. The addition of solar PV capacity to a wind-dominated system results in a significant reduction in the frequency and duration of RES droughts, while also reducing extremes and seasonal RES drought patterns. These findings underscore the importance of diversification in RES capacity to enhance energy security and resilience.

Keywords: RES Drought, Wind Power, Solar PV Power, Renewable Energy Sources, Return Periods

1. Introduction

The EU aims to generate at least 69% of its electricity from renewable energy sources (RES) by 2030, up from 41% in 2022 [1]. While this transition is essential for reducing greenhouse gas emissions, it also highlights the challenge of managing the variability of weather-dependent energy sources such as wind and solar photovoltaic (PV) power. This challenge is amplified by the increasing electrification of energy sectors, which places greater demand on the power system and makes it more sensitive to meteorological conditions, both in historical [2] and future climates [3]. Periods of low renewable generation, known as *Dunkelflaute* or RES droughts, pose significant risks to system adequacy and energy security, emphasising the need for a resilient energy system to meet both growing electricity demand and decarbonisation targets.

RES drought events do not have a fixed definition, with various approaches present in the literature. One common method defines a RES drought as a period during which the average capacity factor (CF) remains below a fixed threshold for a specified duration. For example, Kaspar et al. [4] used this method to investigate the shortfall risks of low wind and solar PV generation in Europe, with a focus on Germany, testing multiple CF thresholds and durations. Similarly, Mockert et al. [5] examined the link between weather regimes and RES droughts in Germany using a 48-hour rolling window under a threshold to define RES droughts. Similar fixed-threshold approaches have also been applied using CF series reconstructed through machine learning in regions such as Japan [6] and Hungary [7].

Alternative methods adjust the CF threshold dynamically over the year to account for seasonal variations in renewable production. Raynaud et al. [8] defined RES droughts as sequences of days with renewable electricity generation below a threshold that varies seasonally, a methodology later adapted for India [9]. Building on this, Kapica et al. [10] compared the likelihood of increased RES droughts in Europe under different climate models. Other studies have defined RES droughts based on deviations from daily mean production: Rinaldi et al. [11] applied these in the U.S. Western Interconnection to quantify the benefits of long-term storage, while Brown et al. [12] examined weekly timescales to explore meteorological influences on the most severe RES drought events. Another method defines RES drought indices based on metrics commonly used in hydro-meteorology to characterise RES droughts [13]. This approach identifies periods of unusually low generation relative to historical production levels, using the lowest production percentiles. Bracken et al. [14] used this approach to analyse RES droughts at different time scales in the U.S. [14], and Lei et al. [15] used it to quantify RES droughts in wind-PV-hydro systems in China.

In addition to examining periods of low renewable electricity generation, several studies also explore the periods when the imbalance between renewable generation and electricity demand (residual demand) is high. Raynaud et al. [8] showed the difference between RES droughts and high residual demand events in a hypothetical fully renewable system composed of wind, solar PV and run-of-the-river hydropower. Similarly, Allen and Otero [13] also defined a standardised index based on meteorological droughts to address residual demand, whose correlation to the electricity generation index is mostly negative (as expected, although quite low anticorrelations and even small positive correlations appear for some European countries). This index

was also applied to the U.S. by Bracken et al. [14], revealing a consistent increase in the RES drought magnitude when demand is considered, despite showing differing results across regions.

In this paper, the focus is exclusively on renewable electricity generation, to keep the focus on RES droughts driven by the weather. A fixed threshold approach is used to define RES droughts, which facilitates consistent inter-comparison between scenarios with different installed wind and solar PV capacities. The case study used in this paper is Ireland, a region where most RES generation comes from wind power and with ambitious targets for solar PV power expansion. This provides valuable insights into the potential benefits of adding solar PV installations in wind-dominated countries.

RES droughts are identified using onshore wind and solar PV CF time series. In this study, three different datasets are used and compared, all of which are driven by the ERA5 reanalysis [16]. Two of the datasets are part of C3S Energy (C3SE), an energy-based operational dataset produced by the EU Copernicus Climate Change Service [17]. One of the C3SE datasets provides CF time series aggregated at the national scale, while the other provides the CF time series at each grid point, at the ERA5 resolution of 0.25° . The third dataset produced by the authors was generated using the Atlite model [18], which converts the ERA5 atmospheric data to a generation time series using specified wind turbine and PV panel models. Atlite is an open-source tool developed by PyPSA [18] and has been used for estimating wind and solar PV generation in order to study RES droughts in Germany [5].

Generic datasets for wind and solar PV CF are often used for the quantification of RES droughts. Despite undergoing a general validation process, they are often not fully representative of each geographical location, and can show differences in the number of RES drought events subsequently identified [19]. This study evaluates the skill of a dataset developed for the European region (C3SE) when applied to a specific country; Ireland. In particular, the analysis explores the impact of using a generic versus a tailored dataset on RES drought assessments, in the context of a transition from a wind-dominated system to one with a greater share of solar PV capacity.

The aim of this study is to answer two questions which are relevant for systems with a large share of RES generation:

- Do generic datasets have sufficient skill to reliably quantify RES drought events for specific countries?
- How does the integration of solar PV capacity into a predominantly

89 wind-based system alter the characteristics of RES drought events?

90 The datasets used in this study are detailed in section 2, which describes
91 their characteristics and relevance for evaluating RES droughts. Section 3
92 outlines the RES datasets used to simulate wind and solar PV generation and
93 provides the methodology for defining and identifying RES drought events,
94 including the thresholds and metrics applied. In section 4, the datasets are
95 first verified against observed energy data to assess their accuracy, followed by
96 an analysis of RES drought occurrences for two scenarios with different ratios
97 of installed wind to solar PV capacities. Finally, section 5 offers a discussion
98 of the results in the context of energy reliability and future planning, followed
99 by the main conclusions and recommendations for further research.

100 2. Data

101 This study uses publicly available datasets to construct and validate the
102 datasets for estimating the CF of wind and solar PV power. The primary
103 data sources include: EirGrid and SONI, the transmission system operators
104 (TSO) for the Republic of Ireland and Northern Ireland, respectively; the
105 ERA5 reanalysis dataset; and the C3SE dataset.

106 2.1. Wind and solar PV Capacity and Availability

107 EirGrid, the TSO for the Republic of Ireland, and SONI, the Northern
108 Ireland TSO, provide detailed datasets on all wind and solar PV farms across
109 the island of Ireland (Republic of Ireland and Northern Ireland) from 1990
110 to the present [20]. These datasets include information such as each farm’s
111 installed capacity, name, and connection date. To enhance the accuracy of
112 this data, the longitude and latitude for each farm were manually determined
113 through online searches. For simplicity, this data will be referred to as orig-
114 inating from EirGrid, as all-island data was directly obtained from EirGrid,
115 and the combined regions of the Republic of Ireland and Northern Ireland
116 will be referred to as Ireland throughout the remainder of this document.

117 The spreadsheet available from the EirGrid website contains two key vari-
118 ables: generation and availability. Generation and availability values are
119 available from 2014 onward for wind power and from 2018 onward for solar
120 PV power, although solar PV availability data only became present in the
121 Republic of Ireland in 2023. Generation is the energy that a RES farm actu-
122 ally contributed to the grid, which may include limitations introduced by the

123 TSO to maintain grid stability, such as constraints and curtailment. Avail-
 124 ability represents the energy that would have been generated from a RES
 125 farm if no grid constraints had been applied, making it representative of the
 126 weather-related response. This study focuses on availability for all analyses.

127 2.2. Atmospheric Variables

128 All of the datasets used in this study are driven by data from the ERA5 re-
 129 analysis [16], produced by the European Centre for Medium-Range Weather
 130 Forecasts (ECMWF). This global gridded dataset provides hourly atmo-
 131 spheric variables from 1940 to the present at a horizontal resolution of 0.25°.
 132 Table 1 lists the relevant ERA5 variables.

Table 1: ERA5 variables used to calculate wind and solar PV generation

ERA5 name	variable
100 metre zonal and meridional wind speed	u_{100}, v_{100}
2 metre temperature	$t2m$
Surface net solar radiation	ssr
Surface solar radiation downwards	$ssrd$
Top of atmosphere incident radiation	$tisr$
Total sky direct solar radiation at surface	$fdir$

133 2.3. C3S Energy

134 The EU Copernicus Climate Change Service developed the C3S-Energy
 135 (C3SE) renewable energy dataset for Europe [17], using ERA5 atmospheric
 136 variables and weather-to-energy models. This dataset provides hourly CF for
 137 wind and solar PV power from 1979 to the present. The data are available
 138 on the same grid as the ERA5 data, which has a horizontal resolution of
 139 0.25°. The time series are also available for download at two aggregated
 140 scales: regional (NUTS 2) and national.

141 The wind CF in C3SE was calculated using wind speeds at 100 metres
 142 (u_{100}, v_{100}) and a standard turbine model, the Vestas V136/3450, with a fixed
 143 hub height of 100 meters. As data on wind turbine fleet locations and speci-
 144 fications are difficult to obtain across Europe, C3SE assumes a homogeneous
 145 distribution of wind turbines across the ERA5 grid. While this approach
 146 does not capture the precise capacity factors reported by grid operators, it
 147 provides a well-correlated time series that effectively represents the impact

of climate variability on wind power generation. The C3SE solar PV CF was also calculated for the ERA5 grid. It is derived from meteorological data, including surface solar radiation downwards (*ssrd*) and air temperature (*t2m*), using a reference solar PV plant model. This model incorporates empirical calculations for key system components such as optical losses, module efficiency, and inverters. The final CF accounts for a mix of module orientations typical for each location [21].

3. Methods

This study analyses RES droughts using onshore wind and solar PV CF time series from three datasets: two from C3SE; one based on national-level data (C3S NAT) and the other on grid-level data (C3S GRD), and a third dataset derived using the Atlite model (ATL).

3.1. C3S Energy National: C3S NAT

The C3S NAT dataset is created by combining two inputs provided by C3SE at the corresponding NUTS levels: Republic of Ireland (NUTS0: IE) and Northern Ireland (NUTS2: UKN0). The two inputs are combined, using the actual installed capacity as weights. This dataset assumes that RES generation occurs at every ERA5 grid point in Ireland.

3.2. C3S Energy Gridded: C3S GRD

The C3S GRD dataset uses, as inputs, the actual locations of the RES farms in Ireland, and the CF from C3SE over the ERA5 grid. For each farm, the CF from the nearest grid point on the C3SE dataset was selected. A weighted average of the CF associated with each farm, using the farm's installed capacities, was used to produce the total CF time series.

3.3. Atlite: ATL

The ATL dataset is produced using the Atlite model. Atlite allows the user to define the wind turbine power curve and PV panel model to use when converting weather variables to wind and solar PV generation. The Atlite model takes as inputs the locations of RES farms and ERA5 weather variables: wind speed at 100 metres (u_{100} , v_{100}) for wind generation, and radiation variables (*ssr*, *ssrd*, *tisr*, and *fdir*) along with air temperature (*t2m*) for solar PV generation. The output of the Atlite model is a generation time series, which is divided by the total capacity to transform it back into

CF. The selection of the wind turbine power curve and PV panel model represents the key difference between this dataset and C3S GRD. This study identifies the most appropriate wind turbine power curve to use from the 121 power curves, each at five different levels of smoothing, made available by Renewables.ninja [22], and selects the PV panel model out of the options available within Atlite.

3.4. Energy Scenarios

The three datasets provide CF time series for both wind and solar PV. In addition to analysing the CF of wind and solar PV separately, a combined CF was computed for each dataset by averaging wind and solar PV CF, weighted by their installed capacities at the end of 2023 (5.9 GW for wind power and 0.6 GW for solar PV power). This configuration is referred to as the 91W-9PV scenario, reflecting the distribution of 91% wind and 9% solar PV capacity. Given that solar PV capacity in Ireland is low in 2023, and to explore how a more balanced distribution of wind and solar PV capacities might impact RES droughts, this study also considered a second scenario, referred to as 57W-43PV, where the installed solar PV capacity is assumed to increase to 8.6 GW, while wind capacity rises to 11.45 GW. These values are based on targets outlined in the roadmap published by the 2024 Climate Action Plan [23]. This study does not include offshore wind in the analysis. Recent reports suggest that even by 2030, Ireland is unlikely to have any significant new offshore wind farms, with projected offshore capacity expected to remain near zero using realistic scenarios [24].

New time series were generated for both the ATL and C3S GRD solar PV datasets, incorporating a revised distribution of installed capacity across Ireland as specified in the roadmap [ADD REFERENCE]. For wind power, the CF time series remains unchanged, as significant shifts in the location of wind farms are not expected. In total, twelve CF time series were analysed in this study, six for individual wind and solar PV CF (three datasets for each source) in the 91W-9PV scenario, and an additional six time series that include the combined CF for 91W-9PV and 57W-43PV scenarios across the different datasets.

It is important to note that the specific capacity values used in this study are illustrative and are not intended to reflect accurate future realities. Instead, they serve to explore the impact of transitioning from a wind-dominated system (91W-9PV) to a more evenly distributed system (57W-43PV). This approach allows for a comparative analysis between the two

218 scenarios, assessing how the balance of RES capacity affects the occurrence
219 of RES droughts.

220 In summary, for each of the three datasets (ATL, C3S GRD and C3S
221 NAT) four energy scenarios are examined:

- 222 • Wind Power - based on the actual capacity at the end of 2023
- 223 • Solar PV Power - based on the actual capacity at the end of 2023
- 224 • Combined RES / 91W-9PV - based on the actual capacity at the end
225 of 2023
- 226 • Combined RES / 57W-43PV - based on the projected capacity for 2030

227 3.5. RES Drought Definition

228 In this study, a RES drought event was defined as occurring when the
229 24-hour moving average of CF remains below a fixed threshold of 0.1 for a
230 period of longer than 24 hours. By using a 24-hour moving average, fewer
231 but longer-lasting events were captured compared to using the raw CF time
232 series, which can be more sensitive to short-term fluctuations. The 24-hour
233 rolling average also avoids potential masking of day-long events due to their
234 start time. A fixed threshold approach was chosen in this study to enable
235 consistent inter-comparison between datasets.

236 The moving average approach smooths out short-term fluctuations, so
237 that brief periods above the threshold do not interrupt an otherwise continu-
238 ous low-CF period (Fig. 1). This means that a single hour above the threshold
239 does not "break" a RES drought event if it is surrounded by prolonged low-
240 generation hours. As a result, fewer but longer-lasting RES drought events
241 are identified, which may better reflect actual conditions where energy supply
242 constraints persist over extended periods.

243 4. Results

244 4.1. Verification

245 The accuracy of the datasets used in this study was verified, before con-
246 tinuing to the analysis of RES droughts. For the verification process, time-
247 varying values of installed capacity were used to account for changes in RES
248 development over the verification period. This step allowed us to assess how

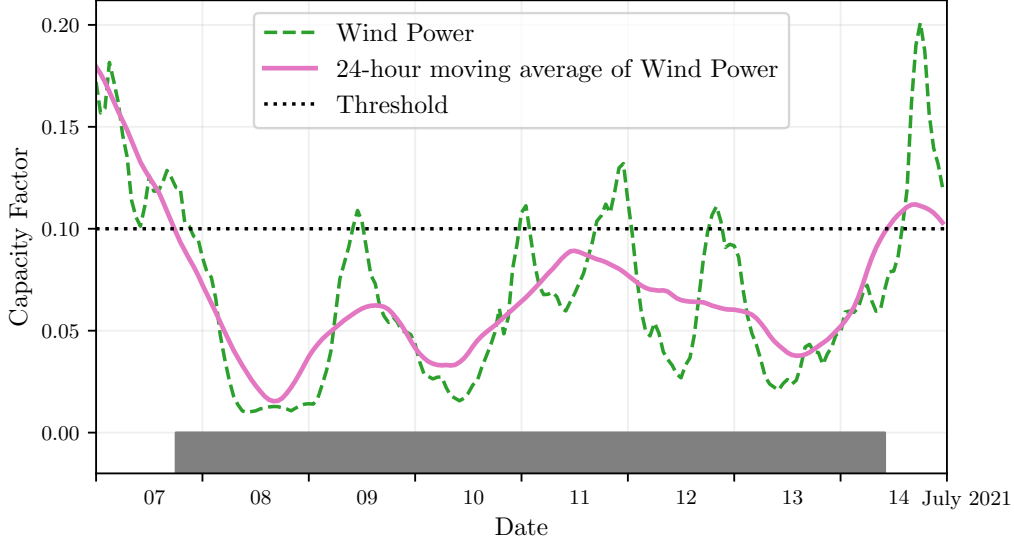


Figure 1: Wind time series of CF (green) and its 24-hour moving average (pink) from the 7th to the 15th of July 2021. The black dashed line indicates the CF threshold. The grey bar shows the period identified as a wind drought under our definition

well the datasets represent the production of renewable energy by comparing them against observed data. This validation step evaluates how well the datasets represent actual renewable energy production by comparing them against observed data. The overall statistical distribution of CF values for wind (2014–2023) and solar PV (2023) is presented in the violin plots in Fig. 2. These plots illustrate the density of CF values for each dataset, highlighting their differences and alignment with observations. The results indicate that ATL aligns more closely with OBS for wind, while all datasets exhibit similar distributions for solar PV.

4.1.1. Wind Energy

The C3S datasets use the Vestas V136/3450 wind turbine power curve (Fig. 3a). The Atlite model allows the user to specify the power curve. We considered the 121 power curves available for download from Renewables.ninja [22]. For each power curve, Renewables.ninja also provides four associated smoothed power curves. The smoothing is done using a Gaussian filter with different standard deviations that depend on the wind speed. A separate wind CF time series for Ireland was generated for each of the wind

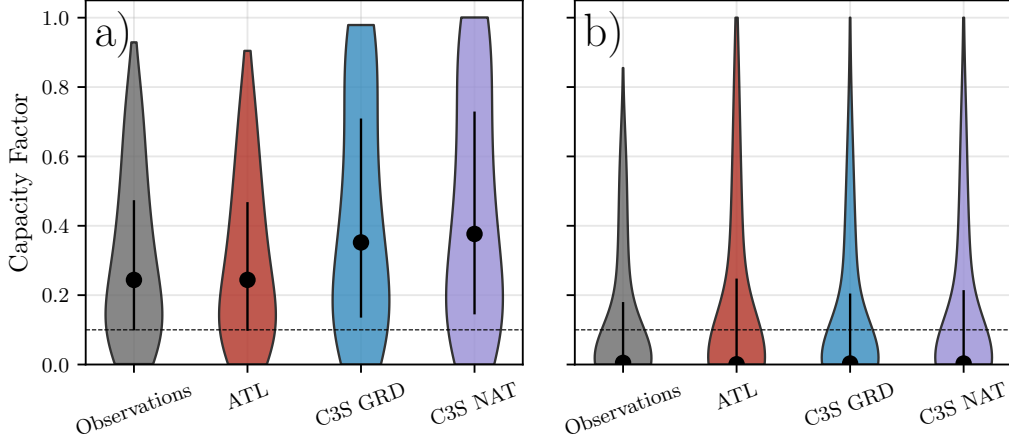


Figure 2: Violin plots of CF distributions for a) wind and b) solar PV for the Observations (grey) and the three datasets: ATL (red), C3S GRD (blue), and C3S NAT (purple). The black dot shows the median values, while the black vertical lines represent the first and third quartiles. The black dashed line indicates the threshold of 0.1 used in the study to identify RES droughts

266 turbine power curves and smoothing levels.

267 The performance of each CF time series is then assessed based on four skill
 268 scores: correlation coefficient (CC), root mean square error (RMSE), mean
 269 bias error (MBE), and the percentage of overlap. The percentage of overlap
 270 quantifies the similarity between the observed and modelled distributions. It
 271 is a positively oriented skill score, where 100% shows full agreement between
 272 the two distributions, and 0% indicates no overlap. The histograms of hourly
 273 CF values for the most recent decade (2014-2023) are used to calculate this
 274 skill score.

275 Based on these metrics, the most representative power curve for Ireland
 276 is the Enercon E112.4500 power curve with the $0.3w$ smoothing filter. The
 277 smoothing of the wind turbine power curve represents losses associated with
 278 each turbine, as well as losses such as wake effects between turbines, which
 279 are important when modelling wind energy on larger spatial scales. The
 280 histogram in Fig. 3b shows that the C3SE power curve tends to underestimate
 281 low CF values and overestimate higher ones, whereas the smoothed ATL
 282 power curve more closely follows the observed wind availability data. This
 283 is further supported by the percentage of overlap which is higher for ATL
 284 (97.2%) than for C3SE (83.2%), indicating better agreement with observed

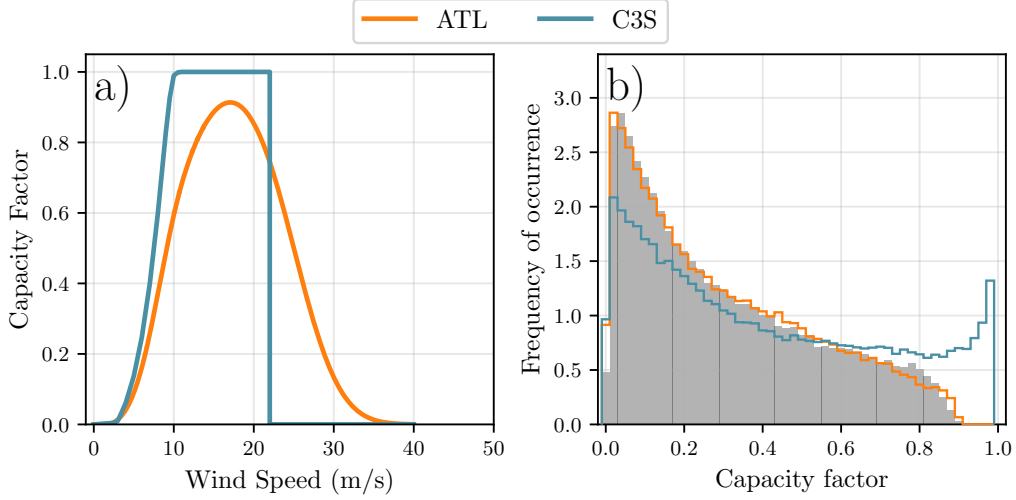


Figure 3: a) Power curves of the Enercon E112.4500 with a 0.3w smoothing filter used by the ATL dataset (orange) and the Vestas V136/3450 used by the two C3S datasets (blue) b) Histograms of wind CF for Ireland for the ATL dataset (orange), the C3S datasets (blue) and Observed (shaded)

285 data.

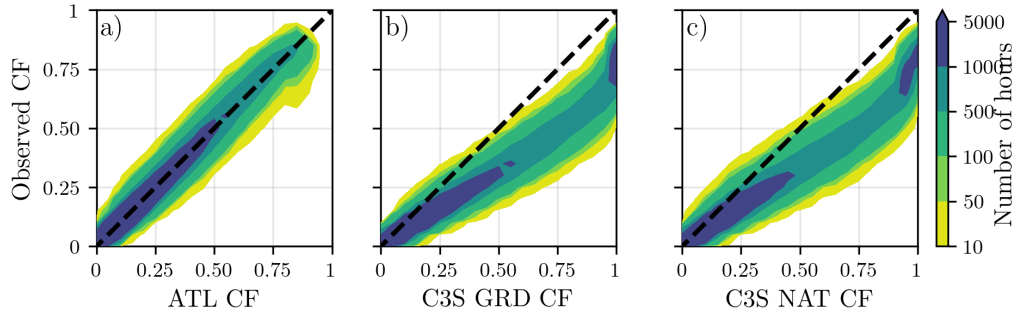


Figure 4: Wind CF density plot of the observed CF (vertical axes) and modelled (horizontal axes) CF data for the a) ATL, b) C3S GRD and c) C3S NAT datasets

286 The effect of the difference between the power curves is also visible in
 287 Fig. 4, which shows a density plot of wind CF values. The two C3S datasets
 288 are shown to overestimate the observed CF, whereas the ATL dataset is in
 289 good agreement with the observed data. The skill scores presented in Table 2

show that ATL performs better than the two C3S datasets for all of the skill scores.

	ATL	C3S GRD	C3S NAT
CC	0.981	0.972	0.970
RMSE	0.045	0.177	0.162
MBE	-0.003	0.137	0.121

Table 2: Skill scores for wind power for the three datasets compared to observed data

Fig. 5 shows the average annual number of wind drought events during the 2014 to 2023 validation period. The figure reveals that ATL presents the best overall agreement with the observed frequency and duration of wind drought events. This pattern is particularly evident for shorter-duration events, which are the most frequent.

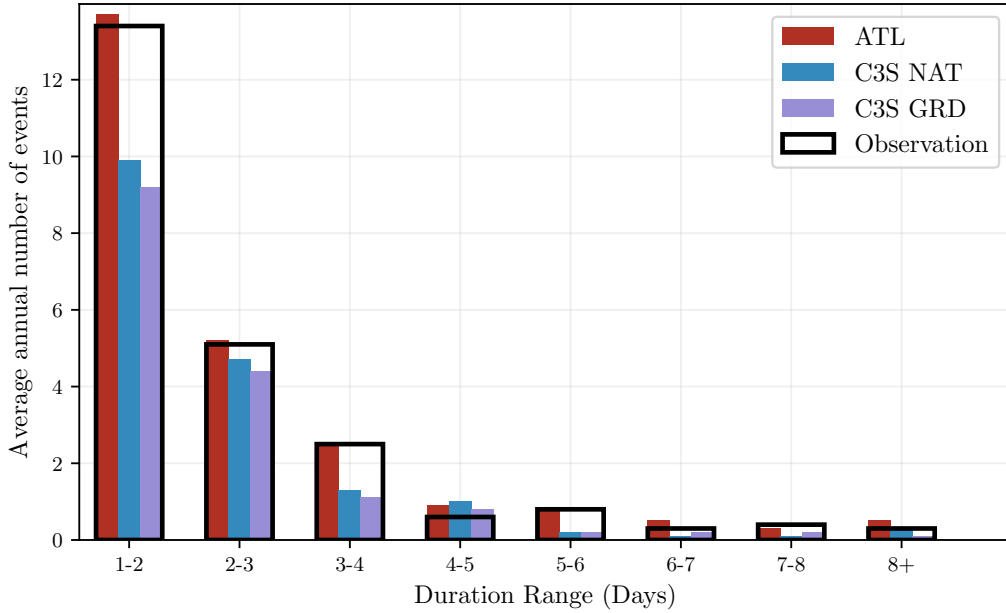


Figure 5: Average annual number of wind drought events for ATL (red), C3S GRD (blue), C3S NAT (purple), and the observed data (black outline). The wind droughts are identified from 2014 to 2023, considering the actual capacity of the system at any given time

This verification for wind generation data highlights the importance of selecting a representative wind turbine power curve for the region being anal-

299 ysed. The ATL dataset, which uses a representative wind turbine power
300 curve, is skilled at reproducing wind CF and RES droughts over Ireland. On
301 the other hand, the power curve used for both C3S GRD and C3S NAT is
302 not representative for Ireland, as it severely overestimates generation, under-
303 estimating the occurrence of RES droughts. This highlights a problem with
304 using generalised datasets for analysing RES droughts: biases severely affect
305 their ability to accurately reproduce RES drought events. The skill scores
306 for the three datasets (Tab. 2) show only a small difference in their ability to
307 reproduce the changes in CF, as seen by their similar CC scores. However,
308 their ability to reproduce the actual CF values is much lower than that of
309 ATL, with RMSE scores almost four times bigger for the two C3S datasets.
310 There is a clear bias towards an overestimation of CF, seen in the MBE val-
311 ues, which leads to the underestimation of RES droughts. This highlights
312 the need to use regionally verified datasets to assess RES droughts.

313 4.1.2. Solar PV Energy

314 The Atlite model allows the user to select certain PV panel characteristics.
315 In this study, the three PV panel types available in the Atlite model were
316 considered (CSi, CdTe, Kaneka). Following the same methodology as in the
317 previous section, the three available models were compared using four skill
318 scores (CC, RMSE, MBE, and the percentage of overlap). Based on the best-
319 performing metrics, the Beyer PV panel model was selected [25], using the
320 Kaneka Hybrid panel option. For all solar PV farm locations, the azimuth
321 angle is fixed at 180°(due south), and the optimal tilt angle option is applied.

322 The solar PV installed capacity available on the spreadsheets from Eir-
323 Grid represents the Maximum Export Capacity (MEC) and does not ac-
324 curately reflect the installed solar PV capacity. To enable actual solar PV
325 generation potential to be modelled correctly, installed capacities were set at
326 1.4 times the MEC values. This scaling factor was estimated by analysing
327 proprietary data from individual solar PV farms provided by EirGrid, which
328 showed that, on average, assuming that the installed capacities of farms ex-
329 ceed their MEC values by 40% yields the best agreement with the observed
330 availability.

331 Fig. 6 shows that the three datasets have a similar tendency to overesti-
332 mate the CF compared to the observed values, especially for high CF values.
333 The skill scores presented in Table 3 indicate that C3S GRD and C3S NAT
334 perform better than ATL for solar PV CF, with lower RMSE and MBE,
335 and higher CC scores. This may be due to the statistical approach taken by

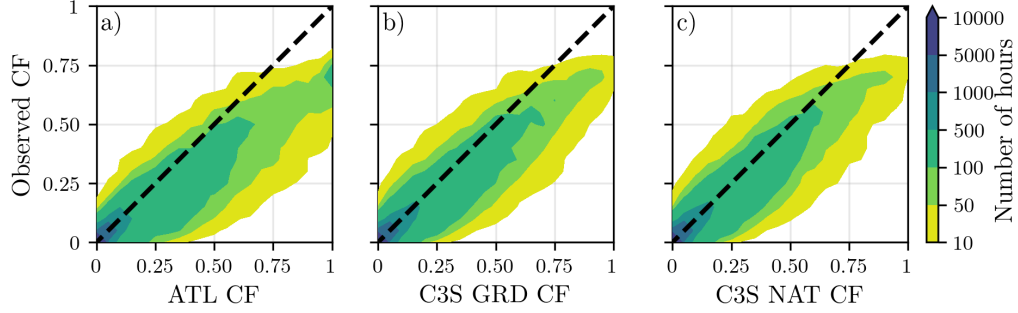


Figure 6: Solar PV CF density plot of the observed (vertical axes) and modelled (horizontal axes) CF series for the a) ATL, b) C3S GRD and c) C3S NAT datasets

336 C3SE for the orientation of the PV panels.

	ATL	C3S GRD	C3S NAT
CC	0.921	0.931	0.931
RMSE	0.119	0.090	0.113
MBE	0.046	0.027	0.021

Table 3: Skill scores for solar PV CF for the three datasets compared to observed data

337 Fig. 7 shows the number of solar PV drought events during the 2023
 338 validation period across different duration ranges. The figure reveals partial
 339 agreement between the three datasets and the observed data, with consistent
 340 results noticed for duration ranges of 1-2, 3-4, 7-8, and 8+ days. However,
 341 discrepancies appear in the other ranges, where the datasets diverge from the
 342 observed data. The main challenge in validating solar PV data stems from
 343 the recent installation of a large share of Ireland’s solar PV capacity, with
 344 over 65% of the total solar PV capacity installed in 2023. This results in
 345 uncertainties in solar PV generation data and the actual generating capacity
 346 in the first few months after each farm is connected. Overall, C3S GRD
 347 performs slightly better than the other datasets in reproducing observed solar
 348 PV drought events.

349 4.2. Analysis

350 In this section, RES droughts are analysed by calculating the frequency
 351 and duration of RES drought events, the return periods for different RES



Figure 7: Number of solar PV drought events for ATL (red), C3S GRD (blue), and C3S NAT (purple) and the observed data (black outline). The solar PV droughts are identified for 2023, considering the actual capacity of the system at any given time

352 drought durations, and the seasonality of RES drought events. Understand-
 353 ing the characteristics and timing of RES drought events enables system op-
 354 erators to optimally plan for reserve capacity requirements, ensuring grid sta-
 355 bility and security of supply. Results are presented for the three datasets, al-
 356 lowing their differences on the characterisation of RES droughts to be clearly
 357 identified.

358 RES drought events are evaluated under two different scenarios with fixed
 359 installed capacities: the 91W-9PV scenario, with 5.9 GW of wind capacity
 360 and 0.6 GW of solar PV capacity; and the 57W-43PV scenario, where wind
 361 capacity comprises 11.45 GW and solar PV capacity increases to 8.6 GW.
 362 Both scenarios were driven by 45 years of ERA5 data. Using the RES drought
 363 identification process described in Section 3.5, wind and solar PV droughts
 364 are first analysed separately before presenting the results for combined (wind
 365 + solar PV) RES droughts under both scenarios.

4.2.1. Annual Number of RES Droughts

The first part of the analysis examines the annual number of RES drought events. When only wind energy is considered (Fig. 8a), the number of RES drought events decreases as the duration range increases, with very few events lasting more than seven days. In contrast, for solar PV energy (Fig. 8b), RES drought frequency declines from one to eight days and then slightly increases for longer durations. This behaviour is attributable to Ireland’s high-latitude location, where reduced sunlight in winter (from November to March) leads to consistently low solar PV output.

Moreover, the comparison between wind and solar PV results indicates that the median, first, and third quartiles for solar PV are consistently higher than or equal to those for wind. This is expected, given that solar PV generation is inherently lower, zero at night, and limited by the solar cycle. When wind and solar PV are combined under the 91W-9PV scenario (Fig. 8c), the results closely mirror those of wind alone, due to the dominance of wind power in the current energy mix. However, in the 57W-43PV scenario (Fig. 8d), a marked reduction in RES drought events is observed across all datasets, with a decrease of the total number of events of 56% for ATL, 52% for C3S GRD, and 50% for C3S NAT, demonstrating the beneficial effects of a more equal share of wind and solar PV capacity.

The consistently higher RES drought counts reported by the ATL dataset, compared to the C3S datasets, underscore the importance of wind turbine power curve representation when quantifying RES droughts. Whereas the three datasets agree on the overall effect of balancing the share of wind and solar PV generation, they differ at a quantitative level, which has crucial implications for energy planning.

4.2.2. Return Periods of RES Drought Duration

RES drought events identified over the 45-year period were used to calculate the return periods for different RES drought durations. A return period is the estimated average time interval between events of a specified duration (not to be confused with the frequency of their occurrence within a fixed time frame). Fig. 9 shows the return periods for different RES drought durations, which can be used to capture the most extreme events affecting the system. Understanding their return periods is crucial, as extreme yet rare RES droughts pose the toughest challenge to energy security by placing significant strain on the conventional backup sources necessary to maintain security of supply during these events.

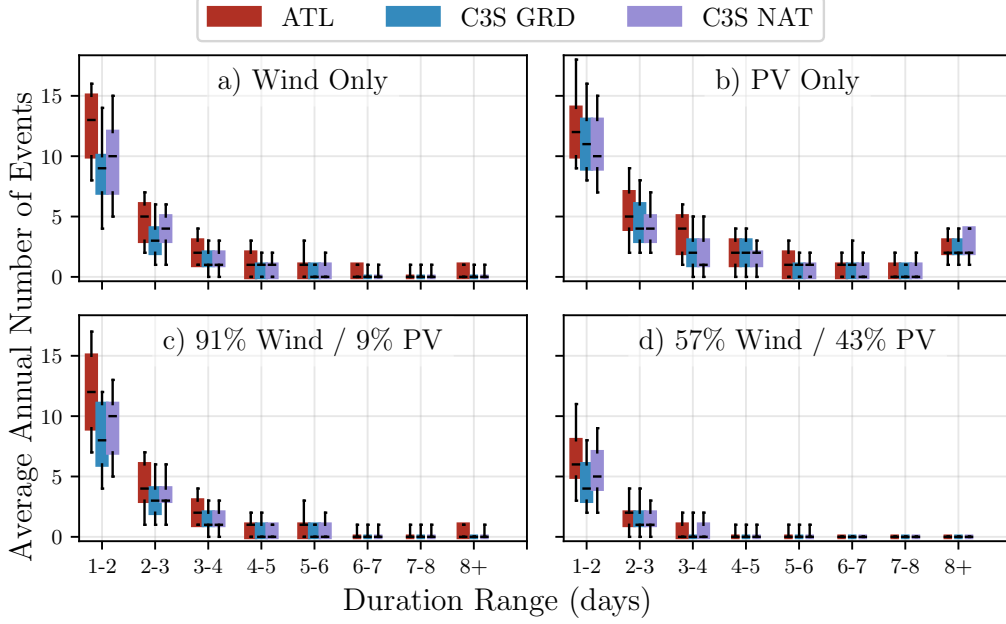


Figure 8: Average annual number of RES droughts (from 1979 to 2023) for a) Wind, b) solar PV, c) 91W-9PV and d) 57W-43PV for ATL (red), C3S GRD (blue), and C3S NAT (purple). The x-axis represents duration ranges in days (lower bound included), while the y-axis indicates the annual number of events. The boxes display the first and third quartiles and the median is marked by a black line. The whiskers indicate the 5th and 95th percentiles

403 The duration of wind droughts (Fig. 9a) increases in a log-linear fashion
404 across the three datasets. The log-linear trend indicates a predictable rela-
405 tionship between wind drought duration and occurrence, with longer wind
406 droughts becoming exponentially less likely as duration increases. In the
407 case of solar PV droughts (Fig. 9b), Atlite behaves differently than the two
408 C3S datasets. The ATL dataset show a generally log-linear increase. For
409 C3S GRD and C3S NAT, the duration of PV droughts increases in a log-
410 linear pattern for events lasting less than 16 days. Beyond this duration,
411 there is a sharp rise in solar PV drought duration for events up to a one-year
412 return period. This sudden increase again reflects the impact of extended
413 periods of low PV generation during winter in Ireland. The difference be-
414 tween the ATL and the C3S results arises from differences in the datasets
415 near the threshold of 0.1 CF. ATL remains slightly above the threshold more

416 frequently during these conditions, leading to shorter, more fragmented RES
417 drought events. In contrast, C3S GRD and C3S NAT tend to fall below the
418 threshold in similar conditions, resulting in longer continuous RES drought
419 periods, especially during winter.

420 Under the 91W-9PV scenario (Fig. 9c), the combined RES drought re-
421 turn periods mirror those for wind alone, reflecting the dominance of wind in
422 the current energy mix. In contrast, the 57W-43PV scenario (Fig. 9d) shows
423 a dramatic reduction in RES drought durations, suggesting that a more bal-
424 anced share of wind and solar PV capacity can substantially mitigate the
425 frequency of prolonged RES drought events. For example, the return pe-
426 riod for a five-day RES drought event (shown by the vertical dashed lines
427 in Fig. 9) increases from roughly six months for the 91W-9PV scenario, to
428 four years for the 57W-43PV scenario in the ATL dataset, and from about
429 fifteen months to around five years in the two C3S datasets. This result in-
430 dicates that the complementarity between wind and solar PV plays a crucial
431 role in reducing the occurrence of RES drought events in a diversified energy
432 portfolio.

433 Across Fig. 9a, c, and d, the return periods in the ATL dataset are con-
434 sistently higher than those in the two C3S datasets. For instance, in the
435 91W-9PV scenario (Fig. 9c), an event with a one-year return period lasts six
436 days in the ATL dataset, compared to only five days in the C3S datasets.
437 This difference underscores the importance of dataset selection when quan-
438 tifying RES droughts, as each dataset’s assumptions and parametrisations
439 significantly influence RES droughts duration estimates. Additionally, in all
440 four graphs, the similarity between results from the two C3S datasets sug-
441 gests that assumptions in the ATL dataset, such as wind turbine power curve
442 selection and PV panel specifications, have a greater impact on RES drought
443 duration estimates than the precise geographic distribution of RES farms
444 when studying the return periods of RES droughts.

445 The return periods calculated from the three datasets show large differ-
446 ences, in particular for the more extreme events with longer return periods.
447 The C3S datasets produce shorter RES drought durations for these events,
448 which would have the largest impact on the power system. This shows that
449 system planning based on the wrong datasets could yield an underestimation
450 of the duration of extreme RES droughts, potentially leading to shortages
451 linked to undersized reserve capacity.

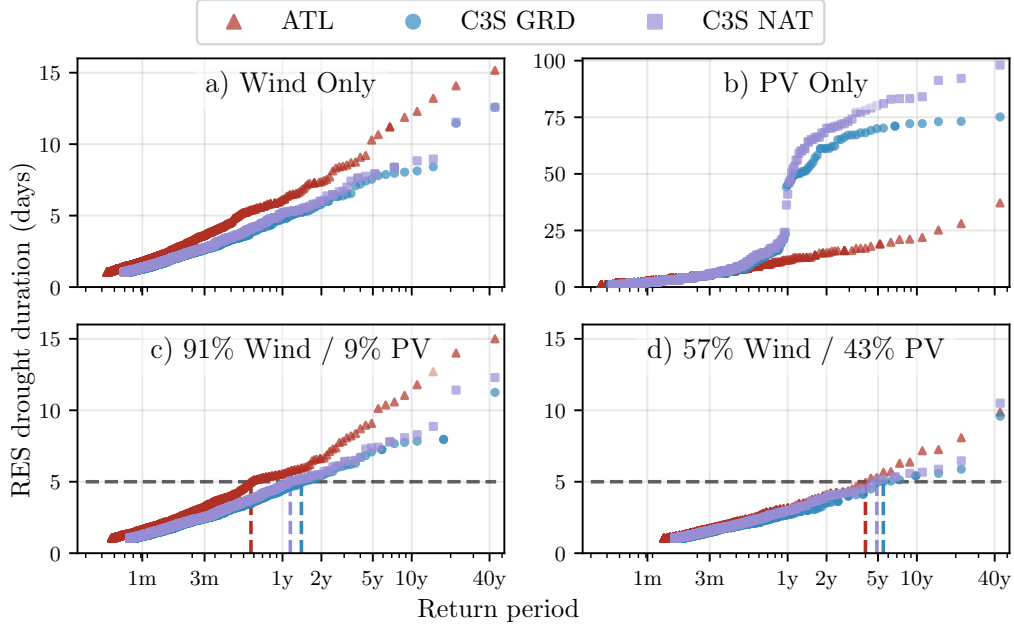


Figure 9: Return periods of the duration of RES droughts (from 1979 to 2023) for a) Wind, b) Solar PV, c) 91W-9PV and d) 57W-43PV for ATL (red triangle), C3S GRD (blue circle), and C3S NAT (purple square). The x-axis represents the return period time in a log-scale and the y-axis indicates the duration of RES drought associated with it. The horizontal dashed line marks the 5-day return period, with coloured vertical dashed marking its return period for each dataset

4.2.3. Seasonal Distribution of RES Droughts

The seasonal analysis of RES droughts is based on the percentage of hours in each month classified as part of a RES drought event. Wind droughts tend to be more frequent during summer, whereas solar PV droughts are more common in winter due to reduced sunlight. By comparing these seasonal patterns across different datasets and energy scenarios, this study examines how dataset-specific assumptions and variations in capacity mix affect the overall characterisation of RES drought events.

For the wind-only scenario (Fig. 10a), the ATL dataset exhibits a pronounced seasonal pattern, with about 24% of summer hours (June, July, August) identified as RES droughts compared to only 4% in winter (December, January, February). This strong seasonal signal is less evident in the C3S datasets, which suggests that the differences in the underlying wind power

465 curves play a significant role. In ATL, CF near or below the 0.1 threshold
 466 occurs at relatively higher wind speeds, resulting in a higher count of RES
 467 drought hours during the summer months. In contrast, solar PV droughts
 468 (Fig. 10b) display an opposite seasonal trend. Across all datasets, over 60%
 469 of winter hours are classified as solar PV droughts, reflecting the naturally
 470 low solar irradiance in Ireland during winter.

471 ATL tends to record a slightly higher percentage of RES drought hours
 472 for wind and a marginally lower percentage for solar PV relative to the C3S
 473 datasets. These differences highlight how dataset-specific assumptions, such
 474 as the treatment of wind turbine power curves and PV panel characteristics,
 475 influences the seasonal dynamics of RES droughts.

476 The 91W-9PV scenario (Fig. 10c) shows patterns similar to the ones for
 477 wind droughts (Fig. 10a). However, in the 91W/9PV scenario, the number
 478 of hours classified as RES droughts in summer decreases slightly compared to
 479 the wind-only scenario. This reduction can be explained by the contribution
 480 of solar PV generation during the summer months in the 91W-9PV scenario,
 481 even though it constitutes only 11% **[SHOULD THIS BE 9%?]** of total
 482 capacity. Since the number of RES drought hours for solar PV in summer is
 483 near zero, this small contribution has a noticeable impact on reducing overall
 484 RES drought hours. In the 57W-43PV scenario (Fig. 10d), all three datasets
 485 show a reduction in monthly RES drought frequency. Annual reductions in
 486 median RES drought frequency are observed across the datasets, dropping
 487 from 14% to 5% for ATL, from 8% to 3% for C3S GRD, and from 9% to 4%
 488 for C3S NAT. The balanced mix of wind and solar PV power in this scenario
 489 reduces the seasonal signal overall and significantly decreases the percentage
 490 of RES drought hours in the summer.

491 The seasonal variations of RES droughts observed in this study have im-
 492 portant implications for energy planning. Energy demand peaks in winter
 493 for Northern European countries, making the seasonality of RES droughts
 494 critical for the sizing of reserve capacity. Our results show that selecting
 495 the wrong dataset could severely underestimate RES droughts during winter
 496 months, thereby affecting the reliability of the energy system during critical
 497 periods. Additionally, the integration of large shares of solar PV in the system
 498 leads to a generalised reduction of RES droughts, yet winter months present
 499 a slight increase. The natural limitations of solar PV lead to inevitably
 500 higher reserve capacity needs during winter months as reliance on RES in-
 501 creases. These types of insights are essential to develop targeted strategies
 502 that enhance grid resilience and ensure a stable energy supply throughout

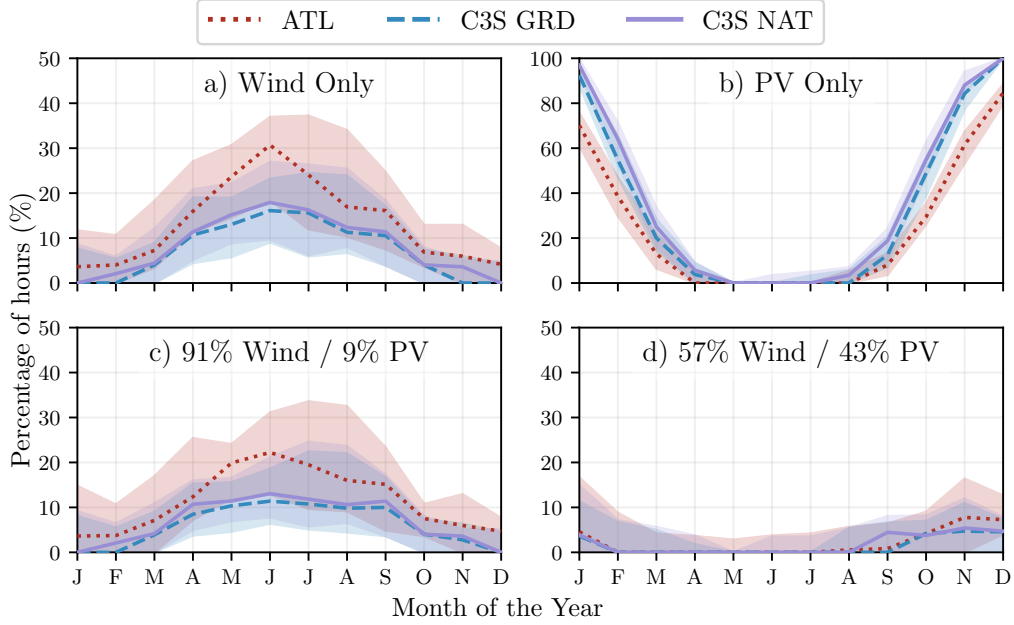


Figure 10: Percentage of hours in a month which are part of a RES drought (from 1979 to 2023) for a) Wind, b) Solar PV, c) 91W-9PV and d) 57W-43PV for ATL (red dotted), C3S GRD (blue dashed), and C3S NAT (purple solid). The x-axis represents the month of the year, and the y-axis indicates the percentage of hours. Lines correspond to the median values and the area between the first and third quartiles is shaded. Note the different y-axis scale for b).

the year.

5. Conclusions

This study aimed to answer two key questions: Do generic datasets have sufficient skill to reliably quantify RES drought events? How does the integration of solar PV into a predominantly wind-based system alter the characteristics of RES droughts? To address these questions, three datasets were compared: two derived from the European C3S-Energy dataset, and one developed by the authors. The datasets derived from C3S-Energy differ in their assumptions, one assumes a homogeneous distribution of wind and solar PV capacity across the region, while the other includes the actual locations of RES farms. The dataset developed by the authors uses a regionally validated

514 model which accounts for farm locations and uses tailored wind and solar PV
515 models selected to represent the actual generation.

516 Our results demonstrate that datasets without regional validation mis-
517 represent the frequency and duration of RES drought events due to their
518 limited ability to reproduce the observations. The inclusion of wind and so-
519 lar PV farm locations has limited impact on RES drought analysis compared
520 to the choice of wind turbine power curves and solar PV models. Whereas
521 all three datasets capture broad trends in the duration and seasonality of
522 RES drought events, the actual number of events is consistently underesti-
523 mated by the non-validated datasets. This effect becomes clearer for extreme
524 events, as not using regionally validated datasets can yield an overestimation
525 of the return periods of RES droughts. This can lead to insufficient reserve
526 capacity planning and potential risks to grid stability and security of supply.

527 The effect of the integration of solar PV capacity in a wind-dominated
528 system on RES droughts has been explored. Our analysis has demonstrated
529 that transitioning to a system with more equal amounts of wind and solar
530 PV capacity reduces the occurrence of RES drought events, mitigates ex-
531 treme RES drought conditions and enhances overall system resilience. This
532 improvement is attributed to the complementary nature of wind and solar
533 PV generation, as solar PV generation typically peaks in summer while wind
534 generation predominates during winter. However, this integration is unable
535 to counter critical winter RES droughts, which coincide with the strongest
536 electricity demand in Northern European countries.

537 The results presented in this study have three main limitations. First,
538 the definition of RES droughts based on generation does not consider the
539 important role of demand, which could be of interest to system operators.
540 Second, recent solar PV capacity expansions have changed the generation
541 profile, limiting solar PV data for model training to a single year, although a
542 longer validation period would be preferable. Third, the source for weather
543 data is ERA5 has limited spatial resolution, an issue that can be addressed
544 once higher resolution datasets become available.

545 Future work is planned to extend the current analysis. First, climate pro-
546 jection data will be integrated with different energy scenarios, incorporating
547 the addition of offshore wind, to better understand how climate change and
548 offshore wind may affect RES droughts. Second, expanding the geographic
549 domain of the study to include the rest of Europe, while also including the
550 role of electricity interconnects between countries, would provide a more com-
551 prehensive understanding of RES droughts. This would require extensive

552 verification across other European countries, making it a more complex but
553 highly relevant challenge.

554 Data Availability

555 The ERA5 data can be obtained from the Climate Data Store (<https://doi.org/10.24381/cds.adbb2d47>). The C3SE dataset is also available
556 from the Climate Data Store (<https://doi.org/10.24381/cds.4bd77450>).
557 Information on wind and solar PV farms in Ireland can be obtained from
558 the EirGrid website (<https://www.eirgrid.ie/grid/system-and-renewable-data-reports>). The Atlite model used in this study is open-source
559 and can be found on GitHub (<https://github.com/pypsa/atlite>). The
560 data and code required to reproduce the analysis in this article will be made
561 available upon acceptance of the manuscript in a public GitHub repository.
562
563

564 Acknowledgments

565 The research conducted in this publication was funded by Science Foun-
566 dation Ireland and co-funding partners under grant number 21/SPP/3756
567 through the NexSys Strategic Partnership Programme.

568 References

- 569 [1] EuroStat, Renewable Energy Statistics, 2023. URL: [https://ec.europa.eu/eurostat/statistics-explained/index.php?title=Renewable](https://ec.europa.eu/eurostat/statistics-explained/index.php?title=Renewable_energy_statistics)
570 [energy_statistics](https://ec.europa.eu/eurostat/statistics-explained/index.php?title=Renewable_energy_statistics), Accessed: 2024-11-06.
571
- 572 [2] H. C. Bloomfield, D. J. Brayshaw, L. C. Shaffrey, P. J. Coker, H. E.
573 Thornton, Quantifying the increasing sensitivity of power systems to
574 climate variability, *Environmental Research Letters* 11 (2016) 124025.
575 doi:10.1088/1748-9326/11/12/124025.
- 576 [3] H. C. Bloomfield, D. J. Brayshaw, A. Troccoli, C. M. Goodess, M. De Fe-
577 lice, L. Dubus, P. E. Bett, Y.-M. Saint-Drenan, Quantifying the
578 sensitivity of european power systems to energy scenarios and cli-
579 mate change projections, *Renewable Energy* 164 (2021) 1062–1075.
580 doi:10.1016/j.renene.2020.09.125.

- 581 [4] F. Kaspar, M. Borsche, U. Pfeifroth, J. Trentmann, J. Drücke, P. Becker,
582 A climatological assessment of balancing effects and shortfall risks of
583 photovoltaics and wind energy in germany and europe, *Advances in*
584 *Science and Research* 16 (2019) 119–128. doi:10.5194/asr-16-119-2
585 019.
- 586 [5] F. Mockert, C. M. Grams, T. Brown, F. Neumann, Meteorological
587 conditions during periods of low wind speed and insolation in Germany:
588 The role of weather regimes, *Meteorological Applications* 30 (2023)
589 e2141. doi:10.1002/met.2141.
- 590 [6] M. Ohba, Y. Kanno, D. Nohara, Climatology of dark doldrums in japan,
591 *Renewable and Sustainable Energy Reviews* 155 (2022) 111927. doi:10
592 .1016/j.rser.2021.111927.
- 593 [7] M. J. Mayer, B. Biró, B. Szücs, A. Aszódi, Probabilistic modeling of
594 future electricity systems with high renewable energy penetration using
595 machine learning, *Applied Energy* 336 (2023) 120801. doi:10.1016/j.
596 apenergy.2023.120801.
- 597 [8] D. Raynaud, B. Hingray, B. François, J. Creutin, Energy droughts from
598 variable renewable energy sources in European climates, *Renewable*
599 *Energy* 125 (2018) 578–589. doi:https://doi.org/10.1016/j.renene
600 .2018.02.130.
- 601 [9] A. Gangopadhyay, A. K. Seshadri, N. J. Sparks, R. Toumi, The role
602 of wind-solar hybrid plants in mitigating renewable energy-droughts,
603 *Renewable Energy* 194 (2022) 926–937. doi:10.1016/j.renene.2022.
604 05.122.
- 605 [10] J. Kapica, J. Jurasz, F. A. Canales, H. Bloomfield, M. Guezgouz,
606 M. De Felice, Z. Kobus, The potential impact of climate change on
607 european renewable energy droughts, *Renewable and Sustainable En-*
608 *ergy Reviews* 189 (2024) 114011. doi:10.1016/j.rser.2023.114011.
- 609 [11] K. Z. Rinaldi, J. A. Dowling, T. H. Ruggles, K. Caldeira, N. S. Lewis,
610 Wind and Solar Resource Droughts in California Highlight the Benefits
611 of Long-Term Storage and Integration with the Western Interconnect,
612 *Environmental Science and Technology* 55 (2021) 6214–6226. doi:10.1
613 021/acs.est.0c07848.

- [12] P. T. Brown, D. J. Farnham, K. Caldeira, Meteorology and climatology of historical weekly wind and solar power resource droughts over western North America in ERA5, *SN Applied Sciences* 3 (2021) 814. doi:10.1007/s42452-021-04794-z.
- [13] S. Allen, N. Otero, Standardised indices to monitor energy droughts, *Renewable Energy* 217 (2023) 119206. doi:10.1016/j.renene.2023.119206.
- [14] C. Bracken, N. Voisin, C. D. Burleyson, A. M. Campbell, Z. J. Hou, D. Broman, Standardized benchmark of historical compound wind and solar energy droughts across the Continental United States, *Renewable Energy* 220 (2024) 119550. doi:<https://doi.org/10.1016/j.renene.2023.119550>.
- [15] H. Lei, P. Liu, Q. Cheng, H. Xu, W. Liu, Y. Zheng, X. Chen, Y. Zhou, Frequency, duration, severity of energy drought and its propagation in hydro-wind-photovoltaic complementary systems, *Renewable Energy* (2024) 120845. doi:10.1016/j.renene.2024.120845, 2.
- [16] H. Hersbach, B. Bell, P. Berrisford, S. Hirahara, A. Horányi, J. Muñoz-Sabater, J. Nicolas, C. Peubey, R. Radu, D. Schepers, et al., The ERA5 global reanalysis, *Quarterly Journal of the Royal Meteorological Society* 146 (2020) 1999–2049. doi:10.1002/qj.3803.
- [17] L. Dubus, Y. Saint-Drenan, A. Troccoli, M. De Felice, Y. Moreau, L. Ho-Tran, C. Goodess, R. Amaro E Silva, L. Sanger, C3S Energy: A climate service for the provision of power supply and demand indicators for Europe based on the ERA5 reanalysis and ENTSO-E data, *Meteorological Applications* 30 (2023) e2145. doi:10.1002/met.2145.
- [18] F. Hofmann, J. Hampp, F. Neumann, T. Brown, J. Hörsch, Atlite: a lightweight Python package for calculating renewable power potentials and time series, *Journal of Open Source Software* 6 (2021) 3294. doi:10.21105/joss.03294.
- [19] A. Kies, B. U. Schyska, M. Bilousova, O. El Sayed, J. Jurasz, H. Stoecker, Critical review of renewable generation datasets and their implications for european power system models, *Renewable and Sustainable Energy Reviews* 152 (2021) 111614. doi:10.1016/j.rser.2021.111614.

- 648 [20] EirGrid & SONI, System and Renewable Data Reports, 2023. URL:
649 [https://www.eirgrid.ie/grid/system-and-renewable-data-rep](https://www.eirgrid.ie/grid/system-and-renewable-data-reports)
650 [orts](https://www.eirgrid.ie/grid/system-and-renewable-data-reports), Accessed: 2024-11-06.
- 651 [21] Y.-M. Saint-Drenan, L. Wald, T. Ranchin, L. Dubus, A. Troccoli, An
652 approach for the estimation of the aggregated photovoltaic power gener-
653 ated in several European countries from meteorological data, *Advances*
654 *in Science and Research* 15 (2018) 51–62. doi:10.5194/asr-15-51-201
655 8.
- 656 [22] I. Staffell, S. Pfenninger, Using bias-corrected reanalysis to simulate
657 current and future wind power output, *Energy* 114 (2016) 1224–1239.
658 doi:10.1016/j.energy.2016.08.068.
- 659 [23] Government of Ireland, Climate Action Plan 2024, Technical Report 3,
660 Department of the Environment, Climate and Communications, 2023.
661 URL: [https://www.gov.ie/pdf/?file=https://assets.gov.ie/](https://www.gov.ie/pdf/?file=https://assets.gov.ie/284675/70922dc5-1480-4c2e-830e-295afd0b5356.pdf)
662 [284675/70922dc5-1480-4c2e-830e-295afd0b5356.pdf](https://www.gov.ie/pdf/?file=https://assets.gov.ie/284675/70922dc5-1480-4c2e-830e-295afd0b5356.pdf), Accessed:
663 2024-11-06.
- 664 [24] Sustainable Energy Authority Ireland, National Energy Projections
665 2024, Technical Report, Sustainability Energy Authority of Ireland,
666 2024. URL: [https://www.seai.ie/news-and-events/news/energ](https://www.seai.ie/news-and-events/news/energy-projections-report)
667 [y-projections-report](https://www.seai.ie/news-and-events/news/energy-projections-report), Accessed: 2024-11-06.
- 668 [25] H. G. Beyer, G. Heilscher, S. Bofinger, A robust model for the mpp
669 performance of different types of pv-modules applied for the performance
670 check of grid connected systems, *Eurosun* (2004) 8.